

The hBUB1 and hBUBR1 kinases sequentially assemble onto kinetochores during prophase with hBUBR1 concentrating at the kinetochore plates in mitosis

S.A. Jablonski¹, G.K.T. Chan¹, C.A. Cooke², W.C. Earnshaw², T.J. Yen¹

¹ Fox Chase Cancer Center, 7701 Burholme Avenue, Philadelphia, PA 19111, USA

² Institute of Cell and Molecular Biology, University of Edinburgh, Michael Swann Building, King's Buildings, Mayfield Road, Edinburgh EH9 3JR, UK

Received: 8 August 1998 / Accepted: 13 September 1998

Abstract. The kinetochore binds an evolutionarily conserved set of checkpoint proteins that function to monitor whether chromosomes have aligned properly at the spindle equator. Human cells contain two related protein kinases, hBUB1 and hBUBR1, that appear to have evolved from a single ancestral BUB1 gene. We generated hBUB1- and hBUBR1-specific antibodies so that the localization patterns of these kinases could be directly compared. In the human U2OS osteosarcoma cell line, hBUB1 first appeared at kinetochores during early prophase before all kinetochores were occupied by hBUBR1 or CENP-F. Both proteins remained at kinetochores throughout mitosis but their staining intensity was reduced from anaphase onward. Kinetochores of unaligned chromosomes exhibited stronger hBUB1 and hBUBR1 staining. Immunoelectron microscopy showed that hBUBR1 appeared to be concentrated in the outer kinetochore plate and in some instances the inner plate as well. When chromosome spreads were examined by light microscopy, hBUB1 and hBUBR1 were coincident with CENP-E. This suggests that both kinases are concentrated near the surface of the kinetochore where they can monitor kinetochore-microtubule interactions.

Introduction

The kinetochore is a macromolecular complex that links chromosomes to the mitotic spindle. The interactions between molecular motors that reside at kinetochores and microtubules of the spindle specify chromosome movements (Schaar et al. 1997; reviewed in Yen and Schaar 1996; Rieder and Salmon 1998). During prometaphase, chromosomes congress toward the spindle equator to form the metaphase plate. Once there, the aligned chromosomes do not normally separate until

the last chromosome achieves alignment at the equator. A mitotic checkpoint can detect the presence of a single unaligned chromosome and delay the onset of anaphase (Rieder et al. 1994). This mechanism ensures that a cell will accurately segregate its chromosomes during anaphase and prevents aneuploidy (reviewed in Elledge 1996). Indeed, a defective checkpoint is thought to be one mechanism that can promote tumor formation (Cahill et al. 1998).

The checkpoint is able to sense whether chromosomes are aligned or not by monitoring kinetochores, whose biochemical composition is believed to change as they progress toward the spindle equator (reviewed in Nicklas 1997; Rieder and Salmon 1998). Thus, an unattached kinetochore emits an undefined inhibitor that prevents premature separation of chromosomes that are aligned (Rieder et al. 1995). In insect spermatocytes, the inhibitory signal appears to be sensitive to the level of tension that is exerted at the kinetochore. When tension is experimentally applied to an unattached kinetochore, the mitotic delay is relieved and the chromosomes that were aligned separate and move poleward (Li and Nicklas 1995). How tension is converted into a signal that is recognized by the checkpoint apparatus is not known. The observation that unattached kinetochores are stained by the 3F3/2 monoclonal antibody (Gorbsky and Ricketts 1993), which recognizes phosphoepitopes on a variety of proteins in mitosis, suggests that certain 3F3/2 phosphoproteins within the kinetochore may generate the inhibitory signal. Indeed, injection of the 3F3/2 antibody into PtK cells prevented dephosphorylation of the phosphoepitope and delayed the onset of anaphase (Campbell and Gorbsky 1995). Interestingly, 3F3/2 phosphorylation was found to be linked to kinetochore tension in grasshopper spermatocytes (Nicklas et al. 1995). The identity of the kinetochore proteins whose 3F3/2 phosphoepitope is sensitive to kinetochore attachment remains to be identified.

The mechanism by which kinetochore-microtubule interactions are transformed into biochemical information that is recognized by the checkpoint apparatus remains

Edited by: W.C. Earnshaw and W. Hennig

Correspondence to: T. Yen
e-mail: tj_yen@fccc.edu

to be determined. However, the identification of an evolutionarily conserved group of mitotic checkpoint proteins has fueled efforts toward this goal. In yeast, the *MAD1*, *MAD2*, *MAD3*, *BUB1*, *BUB2*, *BUB3*, and *MPS1* genes are required for the cell to arrest in mitosis in response to spindle or centromere defects (Hoyt et al. 1991; Li and Murray 1991; Wang and Burke 1995; Pangilinan and Spencer 1996; Weiss and Winey 1996). Bub1 and Bub3 form a protein kinase complex and, along with Mps1 kinase, they function upstream of Mad1 and Mad2 (Roberts et al. 1994; Hardwick and Murray 1995; Hardwick et al. 1996; Wells and Murray 1996). The target of the mitotic checkpoint signal appears to be the cyclosome/anaphase promoting complex (APC), which specifies the degradation of proteins such as Pds1/Cut2 that inhibit anaphase onset (Cohen-Fix et al. 1996; Funabiki et al. 1996; Hwang et al. 1998; Kim et al. 1998).

The discovery of the yeast spindle checkpoint proteins paved the way for the identification of homologous checkpoint components in other species. Vertebrate homologs of Mad1, Mad2, Bub1 and Bub3 were found to be localized at kinetochores during mitosis (Chen et al. 1996; Li and Benezra 1996; Taylor and McKeon 1997; Chan et al. 1998; Cahill et al. 1998; Jin et al. 1998; Taylor et al. 1998). More importantly, Mad2 and Bub1 accumulated to higher levels at unattached versus attached kinetochores (Chen et al. 1996; Li and Benezra 1996; Taylor and McKeon 1997). In the case of Mad2, its accumulation at kinetochores of PtK cells did not appear to be sensitive to tension but rather to the microtubule occupancy of kinetochores (Waters et al. 1998). Functional studies of human and *Xenopus* Mad2 (Chen et al. 1996; Gorbsky et al. 1998; Li and Benezra 1996), and human and mouse BUB1 (Taylor and McKeon 1997; Cahill et al. 1998) showed that they were all required for cells to arrest in mitosis in the presence of spindle defects that were induced by microtubule inhibitors. Consistent with the yeast data, which show that the APC is the target of the checkpoint, *in vitro* experiments show that recombinant Mad2 will inhibit APC activity (Li et al. 1997; Fang et al. 1998). The discovery that these conserved proteins can selectively bind to unattached kinetochores strengthens the notion that these are components of the checkpoint that monitor kinetochore activity during chromosome alignment.

The existence of highly conserved checkpoint proteins suggests that the fundamental mechanism of the checkpoint has also been conserved through evolution. Nevertheless, to accommodate the increased complexity of the structure and functions of mammalian kinetochores, the complexity of the mitotic checkpoint components might also increase. Indeed, human cells express two Bub1-related kinases, hBUB1 and hBUBR1, which were initially identified as mutant genes in some colon carcinomas that exhibited a chromosome instability phenotype (Cahill et al. 1998). hBUB1 and hBUBR1 were also independently isolated from a yeast two-hybrid screen designed to search for interactors with the human kinetochore proteins CENP-F and CENP-E, respectively (Chan et al. 1998; Jablonski and Yen, in preparation). CENP-F is an M_r 367,000 nuclear matrix protein that associates with the nascent kinetochore during late G2 and is proposed

to participate in the early steps of kinetochore assembly (Liao et al. 1995). The interaction seen in yeast between the kinetochore-binding domain of CENP-F and hBUB1 suggests that hBUB1 might also play a part in the kinetochore assembly pathway. CENP-E is a kinetochore motor whose function is essential for chromosome alignment (Schaar et al. 1997; Wood et al. 1997). Kinetochores lacking CENP-E fail to maintain critical kinetochore-microtubule interactions that are important for monopolar chromosomes to establish bipolar connections and for bipolar chromosomes to align at the spindle equator (Schaar et al. 1997). CENP-E forms a complex with hBUBR1 *in vivo* and is postulated to be part of the mechanosensor that links kinetochore motility with the checkpoint (Chan et al. 1998).

Sequence alignment of hBUB1, hBUBR1 and the yeast BUB1 showed that both human BUB1-like kinases were only slightly more similar to each other than they were to yeast BUB1 (Chan et al. 1998; Taylor et al. 1998). This suggested that the two kinases had diverged from the ancestral yeast BUB1 and evolved independently of each other. To investigate the cellular properties of hBUB1 and hBUBR1 in greater detail, we have generated antibodies that specifically recognize either hBUB1 or hBUBR1. In this study, we used these antibodies to compare the distribution patterns of hBUB1 and hBUBR1 in cells as well as at the kinetochore. We found that hBUB1 and hBUBR1 assembled onto kinetochores at different times during prophase. Consistent with vertebrate Mad2 and mouse Bub1, hBUB1 and hBUBR1 staining was stronger at unaligned versus aligned kinetochores. hBUB1 and hBUBR1 staining in metaphase spreads was coincident with CENP-E but bracketed CENP-A, B and C, which were identified with an anti-centromere autoimmune serum (ACA). Immunoelectron microscopy confirmed that hBUBR1 is found in the kinetochore plates where it is ideally positioned to monitor kinetochore-microtubule interactions.

Materials and methods

Cell culture methods. Monolayers of HeLa and U2OS cells were grown at 37°C in Dulbecco's minimal essential medium (DMEM, Gibco BRL, Gaithersburg, Md.) supplemented with 10% fetal calf serum in a humidified 5% CO₂ atmosphere. Cells were plated onto 18 mm glass coverslips and grown to 60% confluency before they were processed for staining.

Immunofluorescence staining. For triple labeling, U2OS and HeLa cells grown on coverslips were extracted in MTSB + 0.5% Triton X-100 (MTSB 4 M glycerol, 0.1 M PIPES pH 6.9, 1 mM EGTA) at room temperature for 1 min, washed in MTSB for 2 min, and then fixed at room temperature for 7 min in 3.5% paraformaldehyde buffered in PBS at pH 6.8. Cells were then washed for 5 min in KB (50 mM TRIS-HCl pH 7.4, 150 mM NaCl, 0.1% BSA). Cells were sequentially stained with affinity-purified rabbit hBUB1 antibodies, rat hBUBR1 antibodies and either monoclonal mouse CENP-E (mAb177) or human autoimmune serum (NR). The rabbit antibodies were detected with a Cy2-conjugated secondary antibody (Jackson ImmunoResearch, West Grove, Pa.), the rat antibodies were biotinylated and detected with Ultra-avidin conjugated to Texas Red (Leinco Technologies, Ballwin, Mo.), and the mouse or human antibodies were detected with Cy5-conjugated secondary antibodies (Jackson

ImmunoResearch). All secondary antibodies had been pre-adsorbed against IgG from other species to prevent cross-reactivity. Nuclei and chromosomes were stained with 4', 6'-diaminophenylindole (DAPI; Sigma) at 0.1 $\mu\text{g}/\text{ml}$. Coverslips were mounted in 0.1% para-phenylenediamine in glycerol and scanned using a Nikon Microphot SA equipped with epifluorescence optics. Cells were visualized with a 100 \times Plan Neofluor objective and images were captured with a TEC-1 CCD camera (DAGE-MTI, Michigan City, Ind.) that was controlled with a Macintosh Quadra 650 running IPLab Spectrum (Signal Analytics, Vienna, Va.). Image processing was performed using Adobe Photoshop 4.0 (Adobe Systems, San Jose, Calif.).

Chromosome spreads were obtained from U2OS cells that had been blocked in 0.5 $\mu\text{g}/\text{ml}$ nocodazole for 14 h. Mitotic cells were collected by shake-off and swollen in 0.8% sodium citrate for 20 min, then dropped onto 12 mm round coverslips and spun at 1,000 g for 2 min. Chromosomes were immediately fixed at room temperature for 7 min in 3.5% paraformaldehyde buffered in PBS at pH 6.8, and processed for staining as described.

Immunoelectron microscopy. HeLa cells were grown in RPMI 1640 supplemented with 10% fetal bovine serum. Mitotic cells were obtained by selective detachment from log-phase cultures, washed in PHEM (60 mM PIPES pH 6.9, 25 mM HEPES, 10 mM EGTA, 2 mM MgCl_2) at room temperature and placed on Adhesion slides (Marienfeld) or polylysine-coated coverslips. Cells were fixed in 4% formaldehyde in PHEM for 5 min at room temperature, then permeabilized by incubation in 0.1% Triton X-100 in PHEM for 5 min at room temperature. After permeabilization, affinity-purified rabbit anti-hBUBR1 was diluted 1:250 in KB^- (10 mM TRIS-HCl, pH 7.7, 150 mM NaCl, 0.1% BSA) and incubated for 1 h at room temperature. After the antibody incubation, the cells were washed (twice for 5 min each) with KB^- and incubated with ultra-small goat anti-rabbit gold (Aurion) in KB^- overnight at 4 $^\circ\text{C}$. The cells were then post-fixed with 2.5% glutaraldehyde in PHEM for 30 min and silver enhanced (Danscher 1981), and processed for electron microscopy as previously described (Cooke et al. 1990). Gold sections were cut with a Reichert microtome and placed on copper grids. Images were photographed on a Philips CM120 Biotwin electron microscope.

Immunoprecipitation. HeLa cells were blocked in 0.5 $\mu\text{g}/\text{ml}$ nocodazole for 14 h, then mitotic cells were collected by shake-off. Asynchronous interphase cells were harvested after mitotic cells had been washed off the plate. Cells were washed three times in ice-cold PBS and lysed in NP-40 buffer (50 mM TRIS-HCl, pH 8.0 150 mM NaCl 1% Nonidet P-40) for 10 min on ice and then scraped into a microfuge tube. Insoluble debris was removed from the lysates by spinning at 14,000 g for 10 min at 4 $^\circ\text{C}$. After determination of the protein concentrations of the lysates (Pierce, Rockford, Ill.), hBUB1 and hBUBR1 rabbit antibodies were incubated with 400 μg of protein from the interphase and mitotic lysates at 4 $^\circ\text{C}$ for several hours. Recombinant protein A-beads (Repligen, Cambridge, Mass.) were added for 1 h, beads were washed five times with NP-40 buffer, samples were boiled in SDS-polyacrylamide gel electrophoresis (SDS-PAGE) sample buffer and separated by 4%–15% SDS-PAGE. The proteins were transferred to Immobilon-P (Millipore, Bedford, Mass.), and incubated with affinity-purified rabbit hBUB1 or hBUBR1 antibodies. After removal of the primary antibodies, filters were incubated with alkaline phosphatase-conjugated secondary antibody (Jackson ImmunoResearch) and processed for detection of chemiluminescence according to the manufacturer's instructions (Tropix, Bedford, Mass.). Blots were stripped according to the manufacturer's instructions (Tropix) and reprobed.

Results

Isolation of hBUB1- and hBUBR1-specific antibodies

To compare the kinetochore localization patterns between hBUB1 and hBUBR1, antibodies were generated to the

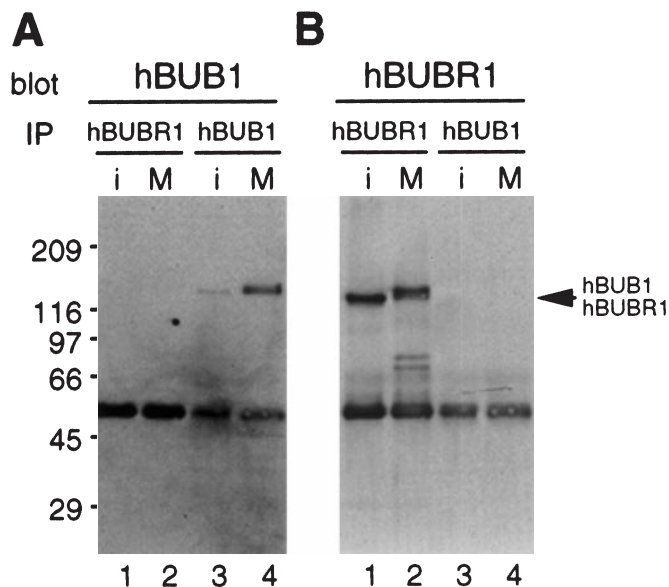


Fig. 1A, B. Specificity of hBUB1 and hBUBR1 antibodies. HeLa lysates from interphase (*i*, lanes 1 and 3) and mitosis (*M*, lanes 2 and 4) were immunoprecipitated with hBUBR1 (lanes 1 and 2) and hBUB1 (lanes 3 and 4) antibodies and blots were probed with either hBUB1 antibodies (A) or hBUBR1 antibodies (B)

portions of hBUB1 and hBUBR1 that were most divergent from each other. Antibodies were generated in rabbits and rats so that hBUB1 and hBUBR1 could be simultaneously visualized by immunofluorescence microscopy. To verify the specificity of the antibodies, the affinity-purified antibodies were used to immunoprecipitate their respective antigens from lysates prepared from either interphase or mitotic HeLa cells. Both the hBUB1 and hBUBR1 immunoprecipitates were then probed with anti-hBUB1 and anti-hBUBR1. The results clearly show that hBUB1 antibodies identified a single band of $\sim M_r$ 130,000 (128,000 calculated) in hBUB1 immunoprecipitates while no cross-reactive band was identified in hBUBR1 immunoprecipitates (Fig. 1A). Likewise, the hBUBR1 antibodies detected an $\sim M_r$ 120,000 protein (calculated 119,000) in the hBUBR1 immunoprecipitates but not in the hBUB1 immunoprecipitates (Fig. 1B). The band that is present in all of the lanes is the IgG that was used for immunoprecipitation. These results show that we have isolated antibodies that specifically recognize hBUB1 and hBUBR1. Furthermore, these results show that the hBUB1 and hBUBR1 that are soluble under the conditions used for the immunoprecipitation are not present in a complex with one another. However, this result does not rule out the possibility that insoluble hBUB1 and hBUBR1 (for example, assembled onto the kinetochore) might be components of a macromolecular complex.

The lower amount of hBUB1 in interphase cells relative to the level found in mitotic cells is due to the fact that the steady-state levels of hBUB1 are low in early stages of interphase and climb to peak levels in mitosis. In contrast, hBUBR1 steady-state levels do not fluctuate

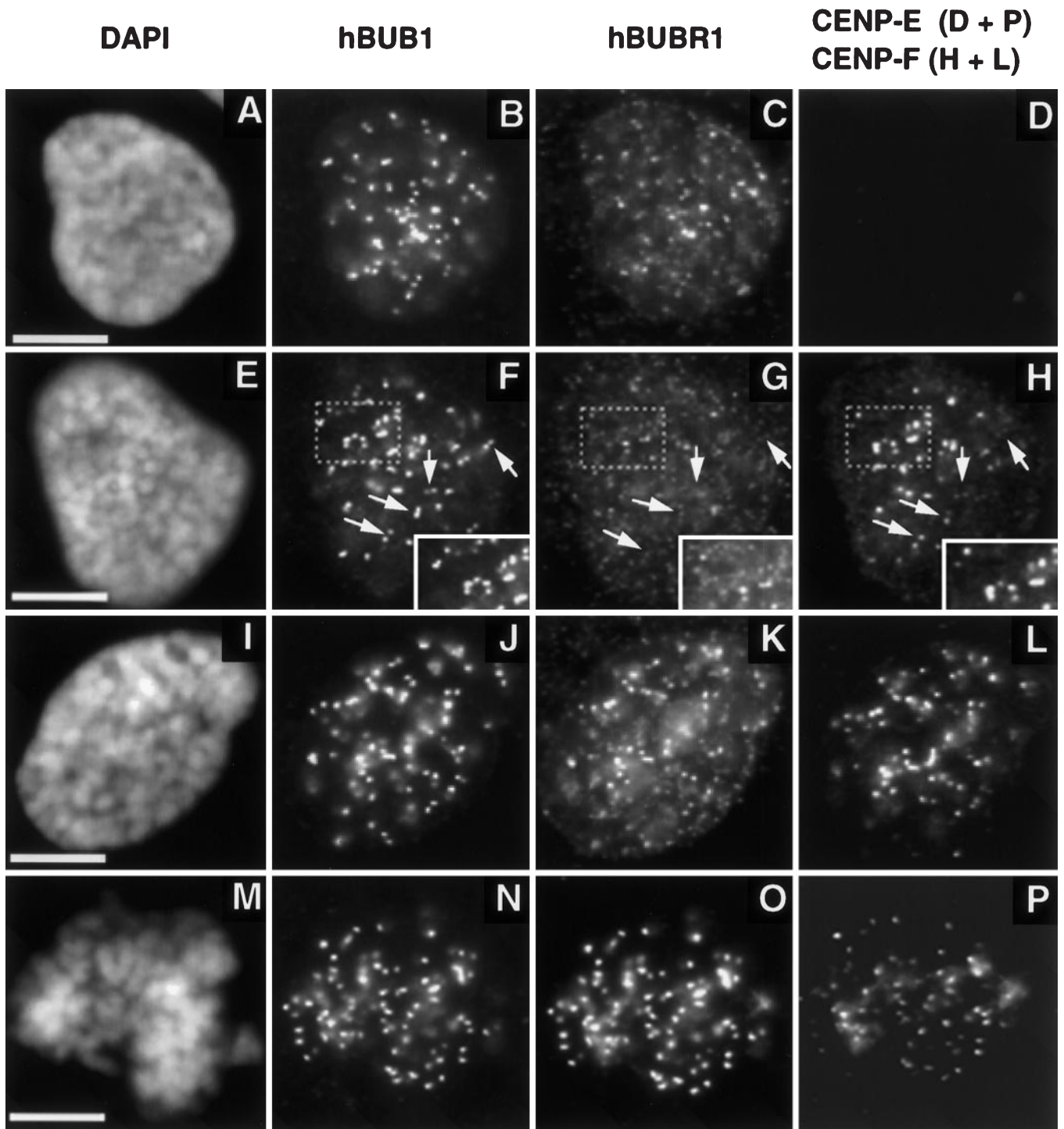
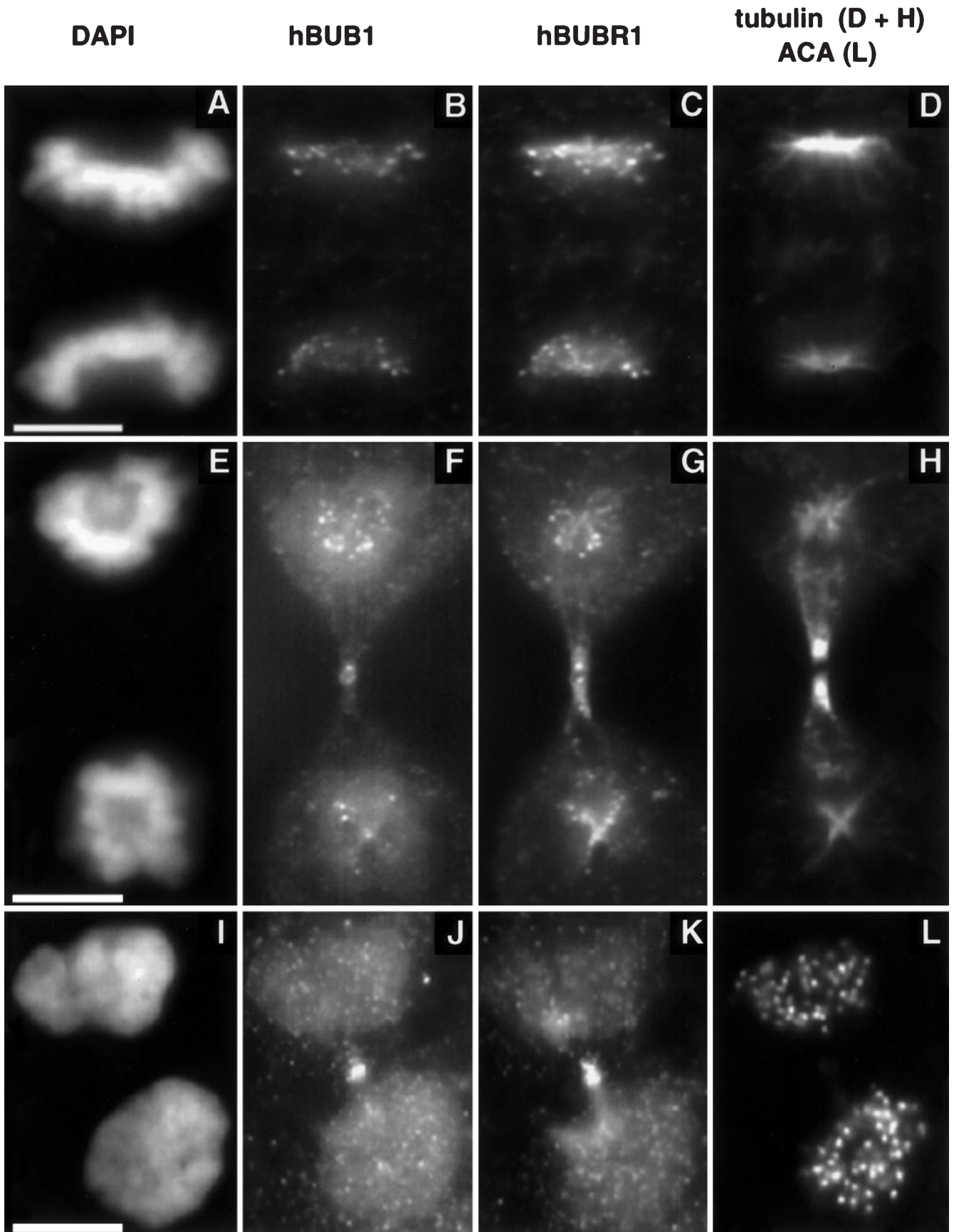


Fig. 2A–P. hBUB1 assembles onto kinetochores before CENP-E and CENP-F in U2OS cells. Cells were sequentially stained with rabbit anti-hBUB1 (**B, F, J, N**), rat anti-hBUBR1 (**C, G, K, O**) and counterstained with Cy2 conjugated anti-rabbit and Texas Red-conjugated anti-rat secondary antibodies, respectively. CENP-E (**D, P**) was detected with a mouse anti-CENP-E monoclonal antibody followed by Cy5-conjugated anti-mouse secondary antibody.

CENP-F (**H, L**) was detected with autoimmune serum (VD) and Cy5-conjugated anti-human secondary antibodies. DNA was stained with 4',6-diamidino-2-phenylindole (DAPI) (**A, E, I, M**). Insets in **F, G** and **H** are higher magnification of the boxed portion of the image that show the differential localization of hBUB1, hBUBR1 and CENP-F. Bar represents 10 μ m



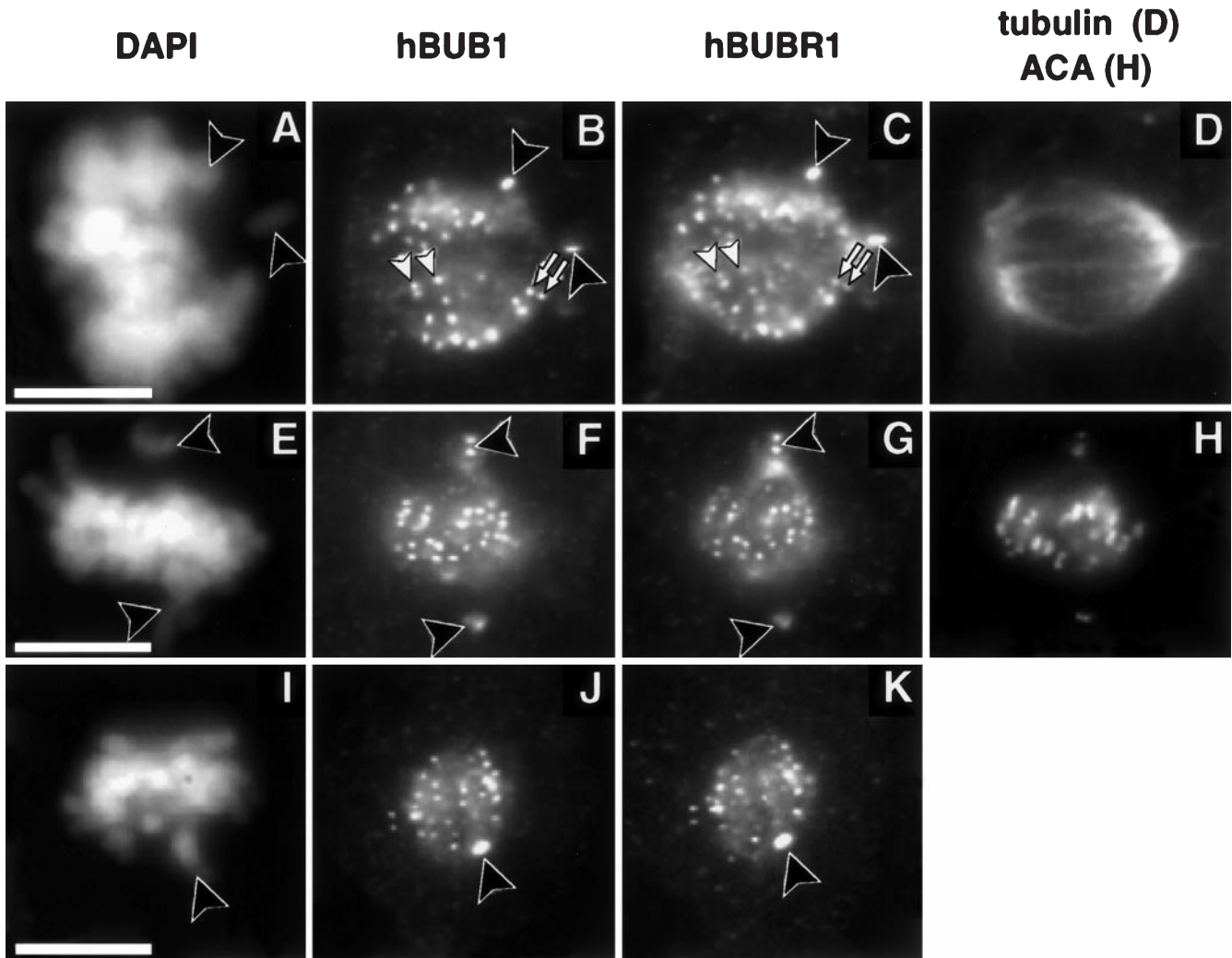


Fig. 4A–K. Unaligned kinetochores of U2OS and HeLa cells exhibit stronger hBUB1 and hBUBR1 staining. U2OS cells with several unaligned chromosomes were stained with hBUB1 (**B, F**), hBUBR1 (**C, G**), and tubulin (**D**) or ACA (**H**). In **B** and **C**, unaligned kinetochores (*white arrows*) are under less tension than aligned kinetochores (*white arrowheads*). HeLa cells with a single unaligned chro-

mosome were stained with hBUB1 (**J**) and hBUBR1 (**K**). Unaligned chromosomes are marked with a *black arrowhead*. hBUB1 and hBUBR1 were visualized with Cy2 and Texas Red secondary antibodies, respectively. Tubulin and ACA were visualized with Cy5 anti-mouse and human secondary antibodies, respectively. *Bar* represents 10 μm

during the cell cycle and thus equivalent amounts of hBUBR1 were expressed in the interphase and mitotic cells (Chan et al. 1998). In mitosis, hBUB1 and hBUBR1 are hyperphosphorylated and this modification retards their migration in SDS-polyacrylamide gels (Chan et al. 1998).

←
Fig. 3A–L. hBUB1 and hBUBR1 are found at the kinetochores until late anaphase but not at telophase. U2OS cells were stained with antibodies against hBUB1 (**B, F, J**), hBUBR1 (**C, G, K**), tubulin (**D, H**) or anti-centromere autoimmune serum (ACA) (**L**). hBUB1 and hBUBR1 were stained as in Fig. 1. Spindles were detected with a monoclonal anti-tubulin antibody and counterstained with Cy5-conjugated anti-mouse secondary antibody. Centromeres were stained with ACA and Cy5-conjugated anti-human secondary antibody. Chromosomes were stained with DAPI (**A, E, I**). *Bar* represents 10 μm

hBUB1 and hBUBR1 bind sequentially to kinetochores

The hBUB1- and hBUBR1-specific antibodies were used to stain the human U2OS osteosarcoma cell line. In interphase cells, hBUB1 was uniformly concentrated in the nucleus in a granular pattern while hBUBR1 was localized primarily in cytoplasm (data not shown). Paired foci of hBUB1 and hBUBR1 staining that were indicative of an association with nascent kinetochores were detected in prophase. Although the intensity of hBUB1 staining was relatively uniform from focus to focus, the intensity of hBUBR1 staining varied (Fig. 2B, C). In addition, a low level of hBUBR1 was also detected that accumulated within the nucleus but was not localized to kinetochores. At this time, CENP-E could not be detected at kinetochores (Fig. 2D).

The difference in the staining patterns for hBUB1 and hBUBR1 during prophase suggested that hBUB1 might

assemble onto the pre-kinetochores prior to hBUBR1. To further delineate the time when these proteins assembled onto kinetochores, we compared their staining pattern with that of CENP-F, a kinetochore protein that was previously shown to appear on nascent kinetochores during late G2 when chromatin condensation is first apparent (Rattner et al. 1993; Liao et al. 1995). In a small number of prophase cells (Fig. 2F, G), we were able to detect relatively uniform hBUB1 staining at the pre-kinetochores (the more dimly stained foci reflect kinetochores that were out of the plane of focus) while hBUBR1 staining of kinetochores was absent or very weak (see inset) even though the protein had accumulated in a granular pattern within the nucleus. Interestingly, certain kinetochores that lacked hBUBR1 staining also lacked detectable CENP-F (Fig. 2H). However, the numbers of pre-kinetochores that exhibited CENP-F staining was greater than those that exhibited hBUBR1 staining. These observations are consistent with an order of binding of the respective proteins as follows: hBUB1→CENP-F→hBUBR1. At a later stage of prophase, all three proteins were colocalized at the pre-kinetochores (Fig. 2I–L) but additional hBUBR1 staining was still detectable throughout the nucleus. By prometaphase, hBUB1, hBUBR1 and CENP-E were all uniformly colocalized at kinetochores (Fig. 2M–P).

hBUB1 and hBUBR1 remain with kinetochores during anaphase

Both human and *Xenopus* Mad2 have been shown to dissociate from kinetochores that are aligned at the spindle equator and do not reassociate with kinetochores when cells enter anaphase (Chen et al. 1996; Li and Benezra 1996). Similarly, mouse Bub1 (homolog of hBUB1) was no longer detectable at kinetochores after onset of anaphase (Taylor and McKeon 1997). Examination of hBUB1 and hBUBR1 staining in U2OS and HeLa cells (not shown) clearly showed that both proteins could be detected at kinetochores up until late anaphase when chromosomes had migrated to the poles (Fig. 3A–D) and were beginning to decondense (Fig. 3E–H). However, the levels of detectable hBUB1 and hBUBR1 at kinetochores in late anaphase were significantly lower than those found during prometaphase. When nuclei reformed and the chromosomes had decondensed during late telophase, hBUB1 and hBUBR1 were no longer detected at kinetochores as determined by co-staining with ACA (Fig. 3I–L) but were concentrated at the midbody. Both proteins were also found dispersed throughout the cytoplasm in a fine granular pattern (that was due most likely to incomplete extraction) but some hBUB1 could be detected in the newly reformed nuclei (Fig. 3J).

hBUB1 and hBUBR1 staining is stronger at kinetochores that are not under tension

We next compared the relative levels of hBUB1 and hBUBR1 at aligned and unaligned kinetochores to assess whether these two proteins responded in the same way

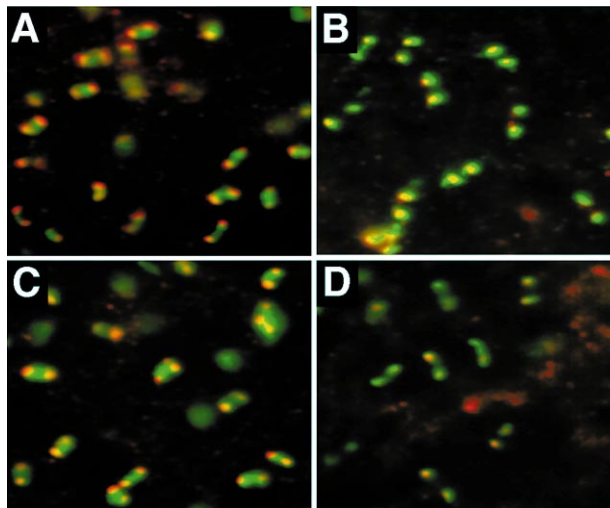


Fig. 5A–D. hBUB1 and hBUBR1 colocalize with CENP-E at kinetochores of metaphase spreads. Metaphase spreads of HeLa cells that were blocked in mitosis with nocodazole were co-stained for hBUB1 and ACA (A), hBUB1 and CENP-E (B), hBUBR1 and ACA (C), and hBUBR1 and CENP-E (D). Images were captured individually, pseudocolored and then overlaid. In A and C, green represents ACA. In B and D, green represents CENP-E. hBUB1 and hBUBR1 are colored red. Regions of overlap appear as yellow

as reported for Mad2 and mouse BUB1. In U2OS cells that contained both aligned and unaligned chromosomes, the intensity of hBUB1 and hBUBR1 staining was noticeably brighter on kinetochores that appeared to be furthest away from the equator (Fig. 4B, C, F and G, open arrowhead). For chromosomes that were within the spindle proper and are thus likely to have established bipolar connections, the hBUB1 and hBUBR1 staining intensities were not noticeably different between kinetochores that were under tension and those that were not. Even though it was difficult to distinguish by DAPI staining whether chromosomes within the spindle were aligned at the metaphase plate or not (Fig. 4A), we were able to estimate the relative tension across the centromere for individual chromosomes based on the distances between sister kinetochores as revealed by hBUB1 and hBUBR1 staining. When kinetochores are under tension their sister kinetochores are maximally separated from each other (Fig. 4, solid arrowheads). When sister kinetochores are not under tension, then the distance between them is less (Fig. 4, solid arrows).

A similar result was obtained when the staining intensities of hBUB1 and hBUBR1 between aligned and unaligned chromosomes in HeLa cells were examined. In the example shown, the hBUB1 and hBUBR1 signal intensity at the kinetochores of a single lagging chromosome is clearly brighter than that of the rest of the kinetochores, which are aligned at the metaphase plate (Fig. 4J, K).

hBUB1 and hBUBR1 colocalize with CENP-E at kinetochores

To ascertain the distribution of hBUB1 and hBUBR1 at kinetochores, metaphase spreads from nocodazole-

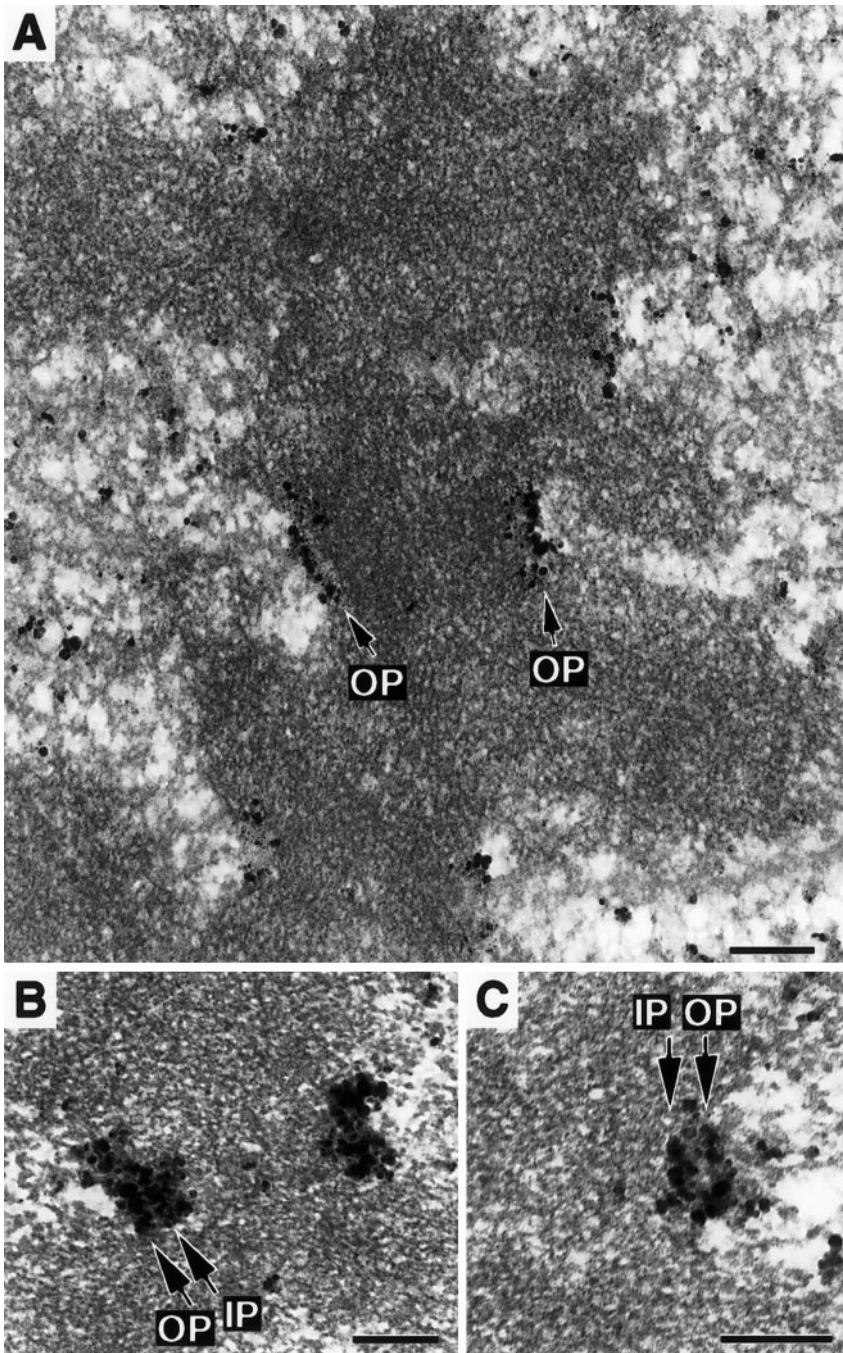


Fig. 6A–C. Immunoelectron microscopy localizes hBUBR1 in the kinetochore plates. **A** hBUBR1 is localized in the outer kinetochore plate (*OP*) in this metaphase cell. **B, C** In other cells, hBUBR1 was localized in two parallel lines that appear to correspond to the inner (*IP*) and outer (*OP*) kinetochore plates. All images show pre-embedding labeling with bound antibody detected using ultra-small colloidal gold. *Bars* represent 0.2 μm

blocked HeLa cells were co-stained for CENP-E, ACA and either hBUB1 or hBUBR1. All kinetochores exhibited uniform levels of staining for all three proteins. When either the hBUB1 or the hBUBR1 image was merged with ACA (Fig. 5A, C, respectively), the two kinases were concentrated at the extreme boundaries flanking the ACA staining pattern. A small amount of overlap between the two images was consistently detected in all of these merged images. When the hBUB1 and hBUBR1 images were merged with CENP-E (Fig. 5B, D, respectively), the staining patterns were coincident. In some examples, CENP-E staining extended beyond the boundary

of the hBUB1 staining (Fig. 5B, green borders). This localization pattern was unaltered when the order of antibody incubation was reversed. Since immunoelectron microscopy studies have localized CENP-E primarily to the fibrous corona coating the outer surface of the outer kinetochore plate (Cooke et al. 1997; Yao et al. 1997), this result suggested that both hBUB1 and hBUBR1 were likely to be concentrated either in the outer kinetochore plate or in the fibrous corona adjacent to CENP-E. This result makes excellent sense, since we have also shown that CENP-E can form a complex with hBUBR1 in mitotic cytosol (Chan et al. 1998).

hBUBR1 is localized at the kinetochore plates

We next used pre-embedding immunoelectron microscopy more precisely to localize hBUBR1 within the kinetochore. For this study, mitotic HeLa cells were obtained by selective detachment in the absence of drug treatment. Most of the cells obtained using this protocol were in metaphase, and in those cells, the most common distribution of gold particles is shown in Fig. 6A. In these chromosomes, the hBUBR1 staining was found in a single line that was coincident with the outer kinetochore plate. If samples were fixed more rapidly after selective detachment, then a higher percentage of prometaphase cells was obtained. Under these conditions, many chromosomes exhibited a strong amorphous staining on the outer surface of the centromere, as shown in the right kinetochore of Fig. 6B. This staining completely obscured the underlying kinetochore substructure. In a number of chromosomes observed under these conditions, the gold particles could be resolved into two parallel lines, as seen in the left kinetochore of Fig. 6B. We interpret this image as showing that hBUBR1 can be concentrated in both the inner and outer plates of the kinetochore. Another example of this is shown in Fig. 6C.

Discussion

We have used antibodies that specifically recognize hBUB1 and hBUBR1 to examine the subcellular distribution of these two related kinases. We found that hBUB1 appears at the nascent kinetochores during late G2 or early prophase, similar to the time when CENP-F is first detected there. However, double-labeling experiments with hBUB1 and CENP-F showed that, in some cells, not all kinetochores that contained hBUB1 exhibited CENP-F staining. We also found cells in which both hBUB1 and CENP-F were uniformly localized to all kinetochores. These observations are consistent with the notion that hBUB1 assembles onto the nascent kinetochores slightly earlier than CENP-F. As yeast two-hybrid studies show that the kinetochore-targeting domain of CENP-F interacts with the kinase domain of hBUB1 (Jablonski and Yen, in preparation), it is possible that CENP-F can only assemble onto the kinetochore when hBUB1 is there. Mechanistically, hBUB1 might phosphorylate CENP-F on residues that are important for kinetochore binding. Alternatively, hBUB1 might phosphorylate other proteins at the kinetochore, which then mediate CENP-F binding. Although it has been shown that hBUB1 is essential for the mitotic checkpoint (Cahill et al. 1998), the protein might also be important for kinetochore assembly. This would be analogous to the dual roles of Mps1 kinase, which is important for spindle pole duplication as well as the spindle checkpoint during mitosis (Weiss and Winey 1996).

Triple-labeling experiments suggested that hBUBR1 assembled onto kinetochores after hBUB1 and CENP-F. However, all of these proteins were found to assemble onto kinetochores before CENP-E, which is first detected at kinetochores after nuclear envelope breakdown. The

combined data are consistent with the existence of a defined kinetochore assembly pathway, with these proteins assembling onto the kinetochore in the following order: hBUB1→CENP-F→hBUBR1→CENP-E.

Examination of mouse Bub1 (homolog of hBUB1) showed that this protein was not detectable at kinetochores after cells had reached metaphase (Taylor and McKeon 1997). Thus, it was somewhat surprising to find that hBUB1 could still be detected at kinetochores during late anaphase when the separated chromatids had reached the poles. As the level of hBUB1 staining was lower in anaphase relative to that seen at prometaphase, it is possible that low amounts of mouse Bub1 at kinetochores during anaphase escaped detection for technical reasons because of the weaker signal strength of the monoclonal antibody used in those studies. Alternatively, the difference in staining pattern between mouse and human might reflect differences in the behavior of the respective BUB1 kinases between the two species. The fact that aligned chromosomes still contain detectable levels of hBUB1 suggests that, for human cells, abrogation of the checkpoint does not require hBUB1 to dissociate completely from aligned kinetochores. This implies either that there is a threshold level of hBUB1 (and possibly hBUBR1) at kinetochores that is required to maintain the checkpoint, or that BUB1 kinases can remain at kinetochores but be switched off.

hBUBR1 was also detected at kinetochores during late anaphase. Like hBUB1, hBUBR1 was no longer detected during telophase when the chromosomes had decondensed and nuclei reformed. The staining pattern of hBUB1 and hBUBR1 at late stages of mitosis is reminiscent of CENP-E, which was also found to remain associated with kinetochores all the way through mitosis (Cooke et al. 1997). Although it is generally believed that hBUB1 and hBUBR1 function during prometaphase to monitor chromosome alignment, this has not formally been demonstrated. The presence of these two kinases at kinetochores during anaphase suggests that they might also have additional roles beyond metaphase. One possibility is that these proteins maintain the integrity of the kinetochore so that other proteins that are important for anaphase chromosome movements can function properly.

The increase in the staining intensity of hBUB1 and hBUBR1 at relaxed (unstretched) kinetochores of chromosomes that are not aligned at the metaphase plate supports their roles as monitors of kinetochore activity during chromosome alignment. Whether the increase in the amount of hBUB1 and hBUBR1 at unaligned kinetochores results from the presence of unoccupied microtubule-binding sites or the lack of tension exerted across the kinetochore remains to be tested. Mad2 was found to be dissociated from kinetochores that were aligned but not under tension (Waters et al. 1998). This suggests that, for Mad2, kinetochore binding might only occur when there are unoccupied microtubule-binding sites. The fact that the kinetochores that lacked tension still retained the 3F3/2 phosphoepitope (Waters et al. 1998), suggests that there are two sets of proteins that separately monitor the level of kinetochore tension and microtubule

occupancy. Consistent with earlier findings, the 3F3/2 phosphoepitope at kinetochores is regulated by tension rather than microtubule occupancy (Nicklas et al. 1995). The checkpoint might only be extinguished when kinetochores are both saturated with microtubules and under a high level of tension.

We have demonstrated elsewhere that hBUBR1 forms a complex with CENP-E in lysates from mitotic cells (Chan et al. 1998). The interactions mediated between the soluble forms of these two proteins might reflect physical interactions at the kinetochore. This possibility has been strengthened by the observation that hBUBR1 and CENP-E staining were coincident at kinetochores. In addition, hBUB1 staining was also found to be coincident with CENP-E.

We have shown by immunoelectron microscopy that hBUBR1 is present in the kinetochore in two different distributions – either in both the inner and outer plates, or concentrated in the outer plate. Although we cannot rigorously correlate these staining patterns with the movements of individual chromosomes during mitosis, one plausible interpretation that is consistent with our results is that when kinetochores are not under tension (metaphase checkpoint is transmitting a signal to delay), then hBUBR1 is present in both the inner and outer kinetochore plates. According to this model, the cessation of kinetochore signaling is associated with either movement of all kinetochore-associated hBUBR1 to the outer plate, or with loss (or epitope masking) of the hBUBR1 from the inner kinetochore plate. The latter hypothesis is most consistent with the decrease in staining intensity seen in metaphase cells relative to prometaphase cells. Ongoing efforts are directed toward the immunoelectron microscopic localization of hBUB1.

This localization of hBUBR1 within the kinetochore makes excellent sense when considered in the light of our knowledge of the binding of CENP-E to the kinetochore. We have shown elsewhere that the kinetochore-targeting region of CENP-E lies near the C-terminus of the protein (Chan et al. 1998). Furthermore, when a construct containing this region of CENP-E was used in a yeast two-hybrid screen to look for interacting molecules, an interaction was seen with hBUBR1. This suggests that hBUBR1 could function to anchor CENP-E to the outer kinetochore plate. Furthermore, this raises the possibility that CENP-E might be the microtubule-binding component of the kinetochore that is responsible for transducing a tension-modulated signal through hBUBR1 to the components of the checkpoint signaling apparatus.

We speculate that hBUBR1 and CENP-E might function as a mechanosensor complex that links kinetochore motility with the checkpoint. It is possible that hBUB1 might monitor CENP-E activity or it might monitor activities of other proteins that reside at the surface of the kinetochore. Regardless of its precise function, the importance of hBUB1 in checkpoint control in humans has been established (Cahill et al. 1998). Further efforts devoted toward elucidating the function of hBUBR1 will help clarify the issue of why there are two Bub1-like kinases in mammalian cells.

Acknowledgements. The authors would like to thank J.C. Hittle for expert assistance in generating antibodies. C.A.C. and W.C.E. were supported by a Principal Research Fellowship from the Wellcome Trust. T.J.Y. was supported by grants from the NIH, American Cancer Society, Leukemia Society Scholar's Award, Council for Tobacco Research, core grant CA06927 and an Appropriation from the Commonwealth of Pennsylvania.

References

- Cahill DP, Lengauer C, Yu J, Riggins GL, Willson JK, Markowitz SD, Kinzler KW, Vogelstein B (1998) Mutations of mitotic checkpoint genes in human cancers. *Nature* 392: 300–303
- Campbell MS, Gorbsky GJ (1995) Microinjection of mitotic cells with the 3F3/2 anti-phosphoepitope antibody delays the onset of anaphase. *J Cell Biol* 129: 1195–1204
- Chan GKT, Schaar BT, Yen TJ (1998) Characterization of the kinetochore binding domain of CENP-E reveals interactions with the kinetochore proteins CENP-F and hBUBR1. *J Cell Biol* 143:49–63
- Chen R-H, Waters JC, Salmon ED, Murray AW (1996) Association of spindle assembly checkpoint component XMD2 with unattached kinetochores. *Science* 274: 242–246
- Cohen-Fix O, Peters JM, Kirschner MW, Koshland D (1996) Anaphase initiation in *Saccharomyces cerevisiae* is controlled by the APC-dependent degradation of the anaphase inhibitor Pds1p. *Genes Dev* 10: 3081–3093
- Cooke CA, Bernat RL, Earnshaw WC (1990) CENP-B: a major human centromere protein located beneath the kinetochore. *J Cell Biol* 110: 1475–1488
- Cooke CA, Schaar B, Yen TJ, Earnshaw WC (1997) Localization of CENP-E in the fibrous corona and outer place of mammalian kinetochores from prometaphase through anaphase. *Chromosoma* 106: 446–455
- Dansch G (1981) Localization of gold in biological tissue: a photochemical method for light and electron microscopy. *Histochemistry* 71: 81–88
- Elledge SJ (1996) Cell cycle checkpoint: preventing an identity crisis. *Science* 274: 1664–1672
- Fang G, Yu H, Kirschner MW (1998) The checkpoint protein MAD2 and the mitotic regulator CDC20 form a ternary complex with the anaphase-promoting complex to control anaphase initiation. *Genes Dev* 12: 1871–1883
- Funabiki H, Yamano H, Kumada K, Nagao K, Hunt T, Yanagida M (1996) Cut2 proteolysis required for sister-chromatid separation in fission yeast. *Nature* 381: 438–441
- Gorbsky GJ, Ricketts WA (1993) Differential expression of a phosphoepitope at the kinetochores of moving chromosomes. *J Cell Biol* 122: 1311–1321
- Gorbsky GJ, Chen R-H, Murray AW (1998) Microinjection of antibody to Mad2 protein into mammalian cells in mitosis induces premature anaphase. *J Cell Biol* 141: 1193–1205
- Hardwick KG, Murray AW (1995) Mad1p, a phosphoprotein component of the spindle assembly checkpoint in budding yeast. *J Cell Biol* 131: 709–720
- Hardwick KG, Weiss E, Luca FC, Winey M, Murray AW (1996) Activation of the budding yeast spindle assembly checkpoint without mitotic spindle disruption. *Science* 273: 953–956
- Hoyt MA, Totis L, Roberts BT (1991) *S. cerevisiae* genes required for cell cycle arrest in response to loss of microtubule functions. *Cell* 66: 507–517
- Hwang LH, Lau LF, Smith DL, Mistrot CA, Hardwick KG, Hwang ES, Amon A, Murray AW (1998) Budding yeast cdc20: a target of a spindle checkpoint. *Science* 279: 1041–1044
- Jin D-Y, Spencer F, Jeang K-T (1998) Human T cell leukemia virus I oncoprotein tax targets the human mitotic checkpoint protein MAD1. *Cell* 93: 81–91
- Kim SH, Lin DP, Matsumoto S, Kitazono A, Matsumoto T (1998) Fission yeast slp1: an effector of the Mad2-dependent spindle checkpoint. *Science* 279: 1045–1047

- Li R, Murray AW (1991) Feedback control of mitosis in budding yeast. *Cell* 66: 519–531
- Li Y, Benzra R (1996) Identification of a human mitotic checkpoint gene: hSMAD2. *Science* 274: 246–248
- Li Y, Gorbea C, Mahaffey D, Rechsteiner M, Benzra R (1997) MAD2 associates with the cyclosome/anaphase-promoting complex and inhibits its activity. *Proc Natl Acad Sci USA* 94: 12431–12436
- Li X, Nicklas RB (1995) Mitotic forces control a cell-cycle checkpoint. *Nature* 373: 630–632
- Liao H, Winkfein RJ, Mack G, Rattner JB, Yen TJ (1995) CENP-F is a protein of the nuclear matrix that assembles onto kinetochores at late G2 and is rapidly degraded after mitosis. *J Cell Biol* 130: 507–518
- Nicklas RB (1997) How cells get the right chromosomes. *Science* 275: 632–637
- Nicklas RB, Ward SC, Gorbisky GJ (1995) Kinetochores are sensitive to tension and may link mitotic forces to a cell cycle checkpoint. *J Cell Biol* 130: 929–939
- Pangilinan F, Spencer F (1996) Abnormal kinetochore structure activates the spindle assembly checkpoint in budding yeast. *Mol Cell Biol* 7: 1195–1208
- Rattner JB, Rao A, Fritzler MJ, Valencia DW, Yen TJ (1993) CENP-F is a ca 400 kDa kinetochore protein that exhibits a cell-cycle dependent localization. *Cell Motil Cytoskeleton* 26: 214–226
- Rieder CL, Salmon ED (1998) The vertebrate cell kinetochore and its roles during mitosis. *Trends Cell Biol* 8: 310–318
- Rieder CL, Schultz A, Cole R, Sluder G (1994) Anaphase onset in vertebrate somatic cells is controlled by a checkpoint that monitors sister kinetochore attachment to the spindle. *J Cell Biol* 127: 1301–1310
- Rieder CL, Cole RW, Khodjakov A, Sluder G (1995) The checkpoint delaying anaphase in response to chromosome monoorientation is mediated by an inhibitory signal produced by unattached kinetochores. *J Cell Biol* 130: 941–948
- Roberts BT, Farr KA, Hoyt MA (1994) The *Saccharomyces cerevisiae* checkpoint gene BUB1 encodes a novel protein kinase. *Mol Cell Biol* 14: 8282–8291
- Schaar BT, Chan GKT, Maddox P, Salmon ED, Yen TJ (1997) CENP-E function at kinetochores is essential for chromosome alignment. *J Cell Biol* 139: 1373–1382
- Taylor SS, McKeon F (1997) Kinetochores: localization of murine Bub1 is required for normal mitotic timing and checkpoint response to spindle damage. *Cell* 89: 727–735
- Taylor SS, Ha E, McKeon F (1998) The human homologue of Bub3 is required for kinetochore localization of Bub1 and a Mad 3/Bub1-related protein kinase. *J Cell Biol* 142: 1–11
- Wang Y, Burke DJ (1995) Checkpoint genes required to delay cell division in response to nocodazole respond to impaired kinetochore function in the yeast *Saccharomyces cerevisiae*. *Mol Cell Biol* 15: 6838–6844
- Waters JC, Chen R-H, Murray AW, Salmon ED (1998) Localization of Mad2 to kinetochores depends on microtubule attachment, not tension. *J Cell Biol* 141: 1181–1191
- Weiss E, Winey M (1996) The *Saccharomyces cerevisiae* spindle pole body duplication gene MPS1 is part of a mitotic checkpoint. *J Cell Biol* 132: 111–123
- Wells WA, Murray AW (1996) Aberrantly segregating centromeres activate the spindle assembly checkpoint in budding yeast. *J Cell Biol* 133:75–84
- Wood KW, Sakowicz R, Goldstein LS, Cleveland DW (1997) CENP-E is a plus end-directed kinetochore motor required for metaphase chromosome alignment. *Cell* 91: 357–366
- Yao X, Anderson KL, Cleveland DW (1997) The microtubule-dependent motor centromere-associated protein E (CENP-E) is an integral component of kinetochore corona fibers that link centromeres to spindle microtubules. *J Cell Biol* 139: 435–447
- Yen TJ, Schaar BT (1996) Kinetochores: molecular motors, switches and gates. *Curr Opin Cell Biol* 8:381–388